Katsaggelos, A.K. “Iterative Image Restoration Algorithms”
Digital Signal Processing Handbook
Ed. Vijay K. Madisetti and Douglas B. Williams
Boca Raton: CRC Press LLC, 1999

34

Iterative Image Restoration Algorithms

Aggelos K. Katsaggelos
Northwestern University

34.1 Introduction

In this chapter we consider a class of iterative restoration algorithms. If $\boldsymbol{y}$ is the observed noisy and blurred signal, $\boldsymbol{D}$ the operator describing the degradation system, $\boldsymbol{x}$ the input to the system, and $\boldsymbol{n}$ the noise added to the output signal, the input-output relation is described by [3, 51]

$$\boldsymbol{y} = \boldsymbol{D}\boldsymbol{x} + \boldsymbol{n}. \tag{34.1}$$

Henceforth, boldface lower-case letters represent vectors and boldface upper-case letters represent a general operator or a matrix. The problem, therefore, to be solved is the inverse problem of recovering $\boldsymbol{x}$ from knowledge of $\boldsymbol{y}$, $\boldsymbol{D}$, and $\boldsymbol{n}$. Although the presentation will refer to and apply to signals of any dimensionality, the restoration of greyscale images is the main application of interest.

There are numerous imaging applications which are described by Eq. (34.1) [3, 5, 28, 36, 52]. $\boldsymbol{D}$, for example, might represent a model of the turbulent atmosphere in astronomical observations with ground-based telescopes, or a model of the degradation introduced by an out-of-focus imaging device. $\boldsymbol{D}$ might also represent the quantization performed on a signal, or a transformation of it, for reducing the number of bits required to represent the signal (compression application).

The success in solving any recovery problem depends on the amount of the available prior information. This information refers to properties of the original signal, the degradation system (which is in general only partially known), and the noise process. Such prior information can, for example, be represented by the fact that the original signal is a sample of a stochastic field, or that the signal is "smooth," or that the signal takes only nonnegative values. Besides defining the amount of prior information, the ease of incorporating it into the recovery algorithm is equally critical.

After the degradation model is established, the next step is the formulation of a solution approach. This might involve the stochastic modeling of the input signal (and the noise), the determination of the model parameters, and the formulation of a criterion to be optimized. Alternatively it might involve the formulation of a functional to be optimized subject to constraints imposed by the prior information. In the simplest possible case, the degradation equation defines directly the solution approach. For example, if $\boldsymbol{D}$ is a square invertible matrix, and the noise is ignored in Eq. (34.1), $\boldsymbol{x} = \boldsymbol{D}^{-1}\boldsymbol{y}$ is the desired unique solution. In most cases, however, the solution of Eq. (34.1) represents an ill-posed problem [56]. Application of regularization theory transforms it to a well-posed problem which provides meaningful solutions to the original problem.

There are a large number of approaches providing solutions to the image restoration problem. For recent reviews of such approaches refer, for example, to [5, 28]. The intention of this chapter is to concentrate only on a specific type of iterative algorithm, the successive approximation algorithm, and its application to the signal and image restoration problem. The basic form of such an algorithm is presented and analyzed first in detail to introduce the reader to the topic and address the issues involved. More advanced forms of the algorithm are presented in subsequent sections.

34.2 Iterative Recovery Algorithms

Iterative algorithms form an important part of optimization theory and numerical analysis. They date back at least to the Gauss years, but they also represent a topic of active research. A large part of any textbook on optimization theory or numerical analysis deals with iterative optimization techniques or algorithms [43, 44]. In this chapter we review certain iterative algorithms which have been applied to solving specific signal recovery problems in the last 15 to 20 years. We will briefly present some of the more basic algorithms and also review some of the recent advances.

A very comprehensive paper describing the various signal processing inverse problems which can be solved by the successive approximations iterative algorithm is the paper by Schafer et al. [49]. The basic idea behind such an algorithm is that the solution to the problem of recovering a signal which satisfies certain constraints from its degraded observation can be found by the alternate implementation of the degradation and the constraint operator. Problems reported in [49] which can be solved with such an iterative algorithm are the phase-only recovery problem, the magnitude-only recovery problem, the bandlimited extrapolation problem, the image restoration problem, and the filter design problem [10]. Reviews of iterative restoration algorithms are also presented in [7, 25]. There are certain advantages associated with iterative restoration techniques, such as [25, 49]: (1) there is no need to determine or implement the inverse of an operator; (2) knowledge about the solution can be incorporated into the restoration process in a relatively straightforward manner; (3) the solution process can be monitored as it progresses; and (4) the partially restored signal can be utilized in determining unknown parameters pertaining to the solution.

In the following we first present the development and analysis of two simple iterative restoration algorithms. Such algorithms are based on a simpler degradation model, when the degradation is linear and spatially invariant, and the noise is ignored. The description of such algorithms is intended to provide a good understanding of the various issues involved in dealing with iterative algorithms. We then proceed to work with the matrix-vector representation of the degradation model and the iterative algorithms. The degradation systems described now are linear but not necessarily spatially invariant. The relation between the matrix-vector and scalar representation of the degradation equation and the iterative solution is also presented. Various forms of regularized solutions and the resulting iterations are briefly presented. As it will become clear, the basic iteration is the basis for any of the iterations to be presented.

34.3 Spatially Invariant Degradation

34.3.1 Degradation Model

Let us consider the following degradation model

$$y(i,j) = d(i,j) * x(i,j)\ , \tag{34.2}$$

where $y(i,j)$ and $x(i,j)$ represent, respectively, the observed degraded and original image, $d(i,j)$ the impulse response of the degradation system, and $*$ denotes two-dimensional (2D) convolution. We rewrite Eq. (34.2) as follows

$$\Phi(x(i,j)) = y(i,j) - d(i,j) * x(i,j) = 0. \tag{34.3}$$

The restoration problem, therefore, of finding an estimate of $x(i,j)$ given $y(i,j)$ and $d(i,j)$ becomes the problem of finding a root of $\Phi(x(i,j)) = 0$.

34.3.2 Basic Iterative Restoration Algorithm

The following identity holds for any value of the parameter β

$$x(i,j) = x(i,j) + \beta\Phi\left(x(i,j)\right)\ . \tag{34.4}$$

Equation (34.4) forms the basis of the successive approximation iteration by interpreting $x(i,j)$ on the left-hand side as the solution at the current iteration step and $x(i,j)$ on the right-hand side as the solution at the previous iteration step. That is,

$$\begin{aligned} x_0(i,j) &= 0 \\ x_{k+1}(i,j) &= x_k(i,j) + \beta\Phi\left(x_k(i,j)\right) \\ &= \beta y(i,j) + (\delta(i,j) - \beta d(i,j)) * x_k(i,j)\ , \end{aligned} \tag{34.5}$$

where $\delta(i,j)$ denotes the discrete delta function and β the relaxation parameter which controls the convergence as well as the rate of convergence of the iteration. Iteration (34.5) is the basis of a large number of iterative recovery algorithms, some of which will be presented in the subsequent sections [1, 14, 17, 31, 32, 38]. This is the reason it will be analyzed in quite some detail. What differentiates the various iterative algorithms is the form of the function $\Phi(x(i,j))$. Perhaps the earliest reference to iteration (34.5) was by Van Cittert [61] in the 1930s. In this case the gain β was equal to one. Jansson et al. [17] modified the Van Cittert algorithm by replacing β with a relaxation parameter that depends on the signal. Also Kawata et al. [31, 32] used Eq. (34.5) for image restoration with a fixed or a varying parameter β.

34.3.3 Convergence

Clearly if a root of $\Phi(x(i,j))$ exists, this root is a *fixed point* of iteration (34.5), that is $x_{k+1}(i,j) = x_k(i,j)$. It is not guaranteed, however, that iteration (34.5) will converge even if Eq. (34.3) has one or more solutions. Let us, therefore, examine under what conditions (sufficient conditions) iteration (34.5) converges. Let us first rewrite it in the discrete frequency domain, by taking the 2D discrete Fourier transform (DFT) of both sides. It should be mentioned here that the arrays involved in iteration (34.5) are appropriately padded with zeros so that the result of 2D circular convolution equals the result of 2D linear convolution in Eq. (34.2). The required padding by zeros determines the size of the 2D DFT. Iteration (34.5) then becomes

$$\begin{aligned} X_0(u,v) &= 0 \\ X_{k+1}(u,v) &= \beta Y(u,v) + (1-\beta D(u,v))\, X_k(u,v)\,, \end{aligned} \tag{34.6}$$

where $X_k(u,v)$, $Y(u,v)$, and $D(u,v)$ represent respectively the 2D DFT of $x_k(i,j)$, $y(i,j)$, and $d(i,j)$, and (u,v) the discrete 2D frequency lattice. We express next $X_k(u,v)$ in terms of $X_0(u,v)$. Clearly,

$$\begin{aligned} X_1(u,v) &= \beta Y(u,v) \\ X_2(u,v) &= \beta Y(u,v) + (1-\beta D(u,v))\, \beta Y(u,v) \\ &= \sum_{\ell=0}^{1} (1-\beta D(u,v))^{\ell}\, \beta Y(u,v) \\ \cdots & \quad \cdots\cdots\cdots \\ X_k(u,v) &= \sum_{\ell=0}^{k-1} (1-\beta D(u,u))^{\ell}\, \beta Y(u,v) \\ &= \frac{1-(1-\beta D(u,v))^k}{1-(1-\beta D(u,v))} \beta Y(u,v) \\ &= (1-(1-\beta D(u,v))^k) X(u,v) \end{aligned} \tag{34.7}$$

if $D(u,v) \neq 0$. For $D(u,v) = 0$,

$$X_k(u,v) = k \cdot \beta Y(u,v) = 0, \tag{34.8}$$

since $Y(u,v) = 0$ at the discrete frequencies (u,v) for which $D(u,v) = 0$. Clearly, from Eq. (34.7) if

$$|1 - \beta D(u,v)| < 1\,, \tag{34.9}$$

then

$$\lim_{k\to\infty} X_k(u,v) = X(u,v)\,. \tag{34.10}$$

Having a closer look at the sufficient condition for convergence, Eq. (34.9), it can be rewritten as

$$\begin{aligned} |1-\beta Re\{D(u,v)\} - \beta Im\{D(u,v)\}|^2 &< 1 \\ \Rightarrow (1-\beta Re\{D(u,v)\})^2 + (\beta Im\{D(u,v)\})^2 &< 1\,. \end{aligned} \tag{34.11}$$

Inequality (34.11) defines the region inside a circle of radius $1/\beta$ centered at $c = (1/\beta, 0)$ in the $(Re\{D(u,v)\}, Im\{D(u,v)\})$ domain, as shown in Fig. 34.1. From this figure it is clear that the left half-plane is not included in the region of convergence. That is, even though by decreasing β the size

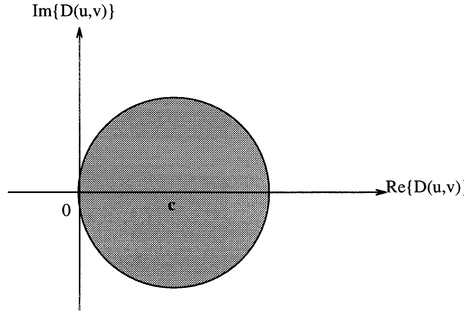

FIGURE 34.1: Geometric interpretation of the sufficient condition for convergence of the basic iteration, where $c = (1/\beta, 0)$.

of the region of convergence increases, if the real part of $D(u, v)$ is negative, the sufficient condition for convergence cannot be satisfied. Therefore, for the class of degradations that this is the case, such as the degradation due to motion, iteration (34.5) is not guaranteed to converge.

The following form of (34.11) results when $Im\{D(u, v)\} = 0$, which means that $d(i, j)$ is symmetric

$$0 < \beta < \frac{2}{D_{\max}(u, v)}\,, \tag{34.12}$$

where $D_{\max}(u, v)$ denotes the maximum value of $D(u, v)$ over all frequencies (u, v). If we now also take into account that $d(i, j)$ is typically normalized, i.e., $\sum_{i,j} d(i, j) = 1$, and represents a low pass degradation, then $D(0, 0) = D_{\max}(u, v) = 1$. In this case (34.11) becomes

$$0 < \beta < 2\,. \tag{34.13}$$

From the above analysis, when the sufficient condition for convergence is satisfied, the iteration converges to the original signal. This is also the inverse solution obtained directly from the degradation equation. That is, by rewriting Eq. (34.2) in the discrete frequency domain

$$Y(u, v) = D(u, v) \cdot X(u, v)\,, \tag{34.14}$$

we obtain, for $D(u, v) \neq 0$,

$$X(u, v) = \frac{Y(u, v)}{D(u, v)}\,. \tag{34.15}$$

An important point to be made here is that, unlike the iterative solution, the inverse solution (34.15) can be obtained without imposing any requirements on $D(u, v)$. That is, even if Eq. (34.2) or (34.14) has a unique solution, that is, $D(u, v) \neq 0$ for all (u, v), iteration (34.5) may not converge if the sufficient condition for convergence is not satisfied. It is not, therefore, the appropriate iteration to solve the problem. Actually iteration (34.5) may not offer any advantages over the direct implementation of the inverse filter of Eq. (34.15) if no other features of the iterative algorithms are used, as will be explained later. The only possible advantage of iteration (34.5) over Eq. (34.15) is that the noise amplification in the restored image can be controlled by terminating the iteration before convergence, which represents another form of regularization. The effect of noise on the quality of the restoration has been studied experimentally in [47]. An iteration which will converge to the inverse solution of Eq. (34.2) for any $d(i, j)$ is described in the next section.

34.3.4 Reblurring

The degradation Eq. (34.2) can be modified so that the successive approximations iteration converges for a larger class of degradations. That is, the observed data $y(i, j)$ are first filtered (reblurred) by a system with impulse response $d^*(-i, -j)$, where * denotes complex conjugation [33]. The degradation Eq. (34.2), therefore, becomes

$$\begin{aligned}\tilde{y}(i, j) = y(i, j) * d^*(-i, -j) &= d^*(-i, -j) * d(i, j) * x(i, j) \\ &= \tilde{d}(i, j) * x(i, j) .\end{aligned} \tag{34.16}$$

If we follow the same steps as in the previous section substituting $y(i, j)$ by $\tilde{y}(i, j)$ and $d(i, j)$ by $\tilde{d}(i, j)$ the iteration providing a solution to Eq. (34.16) becomes

$$\begin{aligned}x_0(i, j) &= 0 \\ x_{k+1}(i, j) &= x_k(i, j) + \beta d^*(-i, -j) * (y(i, j) - d(i, j) * x_k(i, j)) \\ &= \beta d^*(-i, -j) * y(i, j) + (\delta(i, j) \\ &\quad - \beta d^*(-i, -j) * d(i, j)) * x_k(i, j) .\end{aligned} \tag{34.17}$$

Now, the sufficient condition for convergence, corresponding to condition (34.9), becomes

$$|1 - \beta |D(u, v)|^2| < 1 , \tag{34.18}$$

which can be always satisfied for

$$0 < \beta < \frac{2}{\max_{u,v} |D(u, v)|^2} . \tag{34.19}$$

The presentation so far has followed a rather simple and intuitive path, hopefully demonstrating some of the issues involved in developing and implementing an iterative algorithm. We move next to the matrix-vector formulation of the degradation process and the restoration iteration. We borrow results from numerical analysis in obtaining the convergence results of the previous section but also more general results.

34.4 Matrix-Vector Formulation

What became clear from the previous sections is that in applying the successive approximations iteration the restoration problem to be solved is brought first into the form of finding the root of a function (see Eq. (34.3)). In other words, a solution to the restoration problem is sought which satisfies

$$\Phi(\boldsymbol{x}) = 0 , \tag{34.20}$$

where $\boldsymbol{x} \in \mathcal{R}^N$ is the vector representation of the signal resulting from the stacking or ordering of the original signal, and $\Phi(\boldsymbol{x})$ represents a nonlinear in general function. The row-by-row from left-to-right stacking of an image $x(i, j)$ is typically referred to as *lexicographic ordering*.

Then the successive approximations iteration which might provide us with a solution to Eq. (34.20) is given by

$$\begin{aligned}\boldsymbol{x}_0 &= 0 \\ \boldsymbol{x}_{k+1} &= \boldsymbol{x}_k + \beta \Phi(\boldsymbol{x}_k) \\ &= \Psi(\boldsymbol{x}_k) .\end{aligned} \tag{34.21}$$

Clearly if $\boldsymbol{x}^*$ is a solution to $\Phi(\boldsymbol{x}) = 0$, i.e., $\Phi(\boldsymbol{x}^*) = 0$, then $\boldsymbol{x}^*$ is also a fixed point to the above iteration since $\boldsymbol{x}_{k+1} = \boldsymbol{x}_k = \boldsymbol{x}^*$. However, as was discussed in the previous section, even if $\boldsymbol{x}^*$ is the unique solution to Eq. (34.20), this does not imply that iteration (34.21) will converge. This again underlines the importance of convergence when dealing with iterative algorithms. The form iteration (34.21) takes for various forms of the function $\Phi(\boldsymbol{x})$ will be examined in the following sections.

34.4.1 Basic Iteration

From the degradation Eq. (34.1), the simplest possible form $\Phi(\boldsymbol{x})$ can take, when the noise is ignored, is

$$\Phi(\boldsymbol{x}) = \boldsymbol{y} - \boldsymbol{D}\boldsymbol{x} \, . \tag{34.22}$$

Then Eq. (34.21) becomes

$$\begin{aligned} \boldsymbol{x}_0 &= 0 \\ \boldsymbol{x}_{k+1} &= \boldsymbol{x}_k + \beta(\boldsymbol{y} - \boldsymbol{D}\boldsymbol{x}_k) \\ &= \beta\boldsymbol{y} + (\mathbf{I} - \beta\boldsymbol{D})\boldsymbol{x}_k \\ &= \beta\boldsymbol{y} + \mathbf{G}_1\boldsymbol{x}_k \, , \end{aligned} \tag{34.23}$$

where $\mathbf{I}$ is the identity operator.

34.4.2 Least-Squares Iteration

A least-squares approach can be followed in solving Eq. (34.1). That is, a solution is sought which minimizes

$$M(\mathbf{x}) = \|\boldsymbol{y} - \boldsymbol{D}\boldsymbol{x}\|^2 \, . \tag{34.24}$$

A necessary condition for $M(\boldsymbol{x})$ to have a minimum is that its gradient with respect to $\boldsymbol{x}$ is equal to zero, which results in the *normal equations*

$$\boldsymbol{D}^T\boldsymbol{D}\boldsymbol{x} = \boldsymbol{D}^T\boldsymbol{y} \tag{34.25}$$

or

$$\Phi(\boldsymbol{x}) = \boldsymbol{D}^T(\boldsymbol{y} - \boldsymbol{D}\boldsymbol{x}) = 0 \, , \tag{34.26}$$

where ^{T} denotes the transpose of a matrix or vector. Application of iteration (34.21) then results in

$$\begin{aligned} \boldsymbol{x}_0 &= 0 \\ \boldsymbol{x}_{k+1} &= \boldsymbol{x}_k + \beta\boldsymbol{D}^T(\boldsymbol{y} - \boldsymbol{D}\boldsymbol{x}_k) \\ &= \beta\boldsymbol{D}^T\boldsymbol{y} + (\mathbf{I} - \beta\boldsymbol{D}^T\boldsymbol{D})\boldsymbol{x}_k \\ &= \beta\boldsymbol{D}^T\boldsymbol{y} + \mathbf{G}_2\boldsymbol{x}_k \, . \end{aligned} \tag{34.27}$$

It is mentioned here that the matrix-vector representation of an iteration does not necessarily determine the way the iteration is implemented. In other words, the pointwise version of the iteration may be more efficient from the implementation point of view than the matrix-vector form of the iteration.

34.5 Matrix-Vector and Discrete Frequency Representations

When Eqs. (34.22) and (34.26) are obtained from Eq. (34.2), the resulting iterations (34.23) and (34.27), should be identical to iterations (34.5) and (34.17), respectively, and their frequency domain counterparts. This issue, of representing a matrix-vector equation in the discrete frequency domain is addressed next.

Any matrix can be diagonalized using its singular value decomposition. Finding, in general, the singular values of a matrix with no special structure is a formidable task, given also the size of the matrices involved in image restoration. For example, for a 256×256 image, $\boldsymbol{D}$ is of size 64K×64K. The situation is simplified, however, if the degradation model of Eq. (34.2), which represents a special case of the degradation model of Eq. (34.1), is applicable. In this case, the degradation matrix $\boldsymbol{D}$ is block-circulant [3]. This implies that the singular values of $\mathbf{D}$ are the DFT values of $d(i, j)$, and the eigenvectors are the complex exponential basis functions of the DFT. In matrix form, this relationship can be expressed by

$$\boldsymbol{D} = \boldsymbol{W}\tilde{\boldsymbol{D}}\boldsymbol{W}^{-1} , \tag{34.28}$$

where $\tilde{\boldsymbol{D}}$ is a diagonal matrix with entries the DFT values of $d(i, j)$ and $\boldsymbol{W}$ the matrix formed by the eigenvectors of $\boldsymbol{D}$. The product $\boldsymbol{W}^{-1}\boldsymbol{z}$, where $\boldsymbol{z}$ is any vector, provides us with a vector which is formed by lexicographically ordering the DFT values of $z(i, j)$, the unstacked version of $\boldsymbol{z}$. Substituting $\boldsymbol{D}$ from Eq. (34.28) into iteration (34.23) and premultiplying both sides by $\boldsymbol{W}^{-1}$, iteration (34.5) results. The same way iteration (34.17) results from iteration (34.27). In this case, *reblurring*, as was named when initially proposed, is nothing else than the least squares solution to the inverse problem. In general, if in a matrix-vector equation all matrices involved are block circulant, a 2D discrete frequency domain equivalent expression can be obtained. Clearly, a matrix-vector representation encompasses a considerably larger class of degradations than the linear spatially-invariant degradation.

34.6 Convergence

In dealing with iterative algorithms, their convergence, as well as their rate of convergence, are very important issues. Some general convergence results will be presented in this section. These results will be presented for general operators, but also equivalent representations in the discrete frequency domain can be obtained if all matrices involved are block circulant.

The *contraction mapping theorem* usually serves as a basis for establishing convergence of iterative algorithms. According to it, iteration (34.21) converges to a unique fixed point $\boldsymbol{x}^*$, that is, a point such that $\Psi(\boldsymbol{x}^*) = \boldsymbol{x}^*$ for any initial vector if the operator or transformation $\Psi(\boldsymbol{x})$ is a contraction. This means that for any two vectors $\boldsymbol{z}_1$ and $\boldsymbol{z}_2$ in the domain of $\Psi(\boldsymbol{x})$ the following relation holds

$$\|\Psi(z_1) - \Psi(z_2)\| \leq \eta \|z_1 - z_2\| , \tag{34.29}$$

where η is strictly less than one, and $\|\cdot\|$ denotes any norm. It is mentioned here that condition (34.29) is norm dependent, that is, a mapping may be contractive according to one norm, but not according to another.

34.6.1 Basic Iteration

For iteration (34.23) the sufficient condition for convergence (34.29) results in

$$\|\mathbf{I} - \beta\boldsymbol{D}\| < 1, \quad \text{or} \quad \|\mathbf{G}_1\| < 1 . \tag{34.30}$$

If the l_2 norm is used, then condition (34.30) is equivalent to the requirement that

$$\max_i |\sigma_i(\mathbf{G}_1)| < 1 , \tag{34.31}$$

where $|\sigma_i(\mathbf{G}_1)|$ is the absolute value of the i-th singular value of $\mathbf{G}_1$ [54].

The necessary and sufficient condition for iteration (34.23) to converge to a unique fixed point is that

$$\max_i |\lambda_i(\mathbf{G}_1)| < 1, \quad \text{or} \quad \max_i |1 - \beta\lambda_i(\boldsymbol{D})| < 1\,, \tag{34.32}$$

where $|\lambda_i(\boldsymbol{A})|$ represents the magnitude of the i-th eigenvalue of the matrix $\boldsymbol{A}$. Clearly for a symmetric matrix $\boldsymbol{D}$ conditions (34.30) and (34.32) are equivalent. Conditions (34.29) to (34.32) are used in defining the range of values of β for which convergence of iteration (34.23) is guaranteed.

Of special interest is the case when matrix $\boldsymbol{D}$ is singular ($\boldsymbol{D}$ has at least one zero eigenvalue), since it represents a number of typical distortions of interest (for example, distortions due to motion, defocusing, etc). Then there is no value of β for which conditions (34.31) or (34.32) are satisfied. In this case $\mathbf{G}_1$ is a *nonexpansive mapping* (η in (34.29) is equal to one). Such a mapping may have any number of fixed points (zero to infinitely many). However, a very useful result is obtained if we further restrict the properties of $\boldsymbol{D}$ (this results in no loss of generality, as it will become clear in the following sections). That is, if $\boldsymbol{D}$ is a symmetric, semi-positive definite matrix (all its eigenvalues are nonnegative), then according to *Bialy's theorem* [6], iteration (34.23) will converge to the minimum norm solution of Eq. (34.1), if this solution exists, plus the projection of $\boldsymbol{x}_0$ onto the null space of $\boldsymbol{D}$ for $0 < \beta < 2 \cdot \|\boldsymbol{D}\|^{-1}$. The theorem provides us with the means of incorporating information about the original signal into the final solution with the use of the initial condition.

Clearly, when $\boldsymbol{D}$ is block circulant the conditions for convergence shown above can be written in the discrete frequency domain. More specifically, conditions (34.31) and (34.9) are identical in this case.

34.6.2 Iteration with Reblurring

The convergence results presented above also holds for iteration (34.27), by replacing $\mathbf{G}_1$ by $\mathbf{G}_2$ in expressions (34.30) to (34.32). If $\boldsymbol{D}^T\boldsymbol{D}$ is singular, according to Bialy's theorem, iteration (34.27) will converge to the minimum norm least squares solution of (34.1), denoted by $\boldsymbol{x}^+$, for $0 < \beta < 2 \cdot \|\boldsymbol{D}\|^{-2}$, since $\boldsymbol{D}^T\boldsymbol{y}$ is in the range of $\boldsymbol{D}^T\boldsymbol{D}$.

The rate of convergence of iteration (34.27) is linear. If we denote by $\boldsymbol{D}^+$ the *generalized inverse* of $\boldsymbol{D}$, that is, $\boldsymbol{x}^+ = \boldsymbol{D}^+\boldsymbol{y}$, then the rate of convergence of (34.27) is described by the relation [26]

$$\frac{\|\boldsymbol{x}_k - \boldsymbol{x}^+\|}{\|\boldsymbol{x}^+\|} \le c^{k+1}\,, \tag{34.33}$$

where

$$c = \max\{\, |1 - \beta\|\boldsymbol{D}\|^2|, \;\; |1 - \beta\|\boldsymbol{D}^+\|^{-2}|\,\}\,. \tag{34.34}$$

The expression for c in (34.34) will also be used in Section 34.8, where higher order iterative algorithms are presented.

34.7 Use of Constraints

Iterative signal restoration algorithms regained popularity in the 1970s due to the realization that improved solutions can be obtained by incorporating prior knowledge about the solution into the restoration process. For example, we may know in advance that $\boldsymbol{x}$ is bandlimited or space-limited, or we may know on physical grounds that $\boldsymbol{x}$ can only have nonnegative values. A convenient way of expressing such prior knowledge is to define a constraint operator $\mathcal{C}$, such that

$$\boldsymbol{x} = \mathcal{C}\boldsymbol{x}\,, \tag{34.35}$$

if and only if $\boldsymbol{x}$ satisfies the constraint. In general, $\mathcal{C}$ represents the concatenation of constraint operators. With the use of constraints, iteration (34.21) becomes [49]

$$\begin{aligned} \boldsymbol{x}_0 &= 0, \\ \tilde{\boldsymbol{x}}_k &= \mathcal{C}\boldsymbol{x}_k, \\ \boldsymbol{x}_{k+1} &= \Psi(\tilde{\boldsymbol{x}}_k) . \end{aligned} \tag{34.36}$$

The already mentioned recent popularity of constrained iterative restoration algorithms is also due to the fact that solutions to a number of recovery problems, such as the bandlimited extrapolation problem [48, 49] and the reconstruction from phase or magnitude problem [49, 57], were provided with the use of algorithms of the form (34.36) by appropriately describing the distortion and constraint operators. These operators are defined in the discrete spatial or frequency domains. A review of the problems which can be solved by an algorithm of the form of (34.36) is presented by Schafer et al. [49].

The contraction mapping theorem can again be used as a basis for establishing convergence of constrained iterative algorithms. The resulting sufficient condition for convergence is that at least one of the operators $\mathcal{C}$ and Ψ is contractive while the other is nonexpansive. Usually it is harder to prove convergence and determine the convergence rate of the constrained iterative algorithm, taking also into account that some of the constraint operators are nonlinear, such as the positivity constraint operator.

34.7.1 The Method of Projecting Onto Convex Sets (POCS)

The method of POCS describes an alternative approach in incorporating prior knowledge about the solution into the restoration process. It reappears in the engineering literature in the early 1980s [64], and since then it has been successfully applied to the solution of different restoration problems (from the reconstruction from phase or magnitude [52] to the removal of blocking artifacts [62, 63], for example). According to the method of POCS the incorporation of prior knowledge into the solution can be interpreted as the restriction of the solution to be a member of a closed convex set that is defined as the set of vectors which satisfy a particular property. If the constraint sets have a nonempty intersection, then a solution that belongs to the intersection set can be found by the method of POCS. Indeed, any solution in the intersection set is consistent with the *a priori* constraints and, therefore, it is a feasible solution.

More specifically, let $Q_1, Q_2, \cdots, Q_m$ be closed convex sets in a finite dimensional vector space, with $\boldsymbol{P}_1, \boldsymbol{P}_2, \cdots, \boldsymbol{P}_m$ their respective projectors. Then, the iterative procedure,

$$\boldsymbol{x}_{k+1} = \boldsymbol{P}_1\boldsymbol{P}_2 \cdots \boldsymbol{P}_m\boldsymbol{x}_k , \tag{34.37}$$

converges to a vector which belongs to the intersection of the sets Q_i, $i = 1, 2, \cdots, m$, for any starting vector $\boldsymbol{x}_0$. It is interesting to note that the resulting set intersection is also a closed convex set.

Clearly, the application of a projection operator $\boldsymbol{P}$ and the constraint $\mathcal{C}$, discussed in the previous section, express the same idea. Projection operators represent nonexpansive mappings.

34.8 Class of Higher Order Iterative Algorithms

One of the drawbacks of the iterative algorithms presented in the previous sections is their linear rate of convergence. In [26] a unified approach is presented in obtaining a class of iterative algorithms with different rates of convergence, based on a representation of the generalized inverse of a matrix. That is, the algorithm,

$$\boldsymbol{x}_0 = \beta \boldsymbol{D}^T \boldsymbol{y}$$

$$\begin{aligned}\boldsymbol{D}_0 &= \beta \boldsymbol{D}^T \boldsymbol{D} \\ \Omega_{k+1} &= \sum_{i=0}^{p-1} (\mathbf{I} - \boldsymbol{D}_k)^i \\ \boldsymbol{D}_{k+1} &= \Omega_k \boldsymbol{D}_k \\ \boldsymbol{x}_{k+1} &= \Omega_k \boldsymbol{x}_k \,,\end{aligned} \tag{34.38}$$

converges to the minimum norm least squares solution of Eq. (34.1), with $\boldsymbol{n} = 0$. If iteration (34.38) is thought of as corresponding to iteration (34.27), then an iteration similar to (34.38) which corresponds to iteration (34.23) has also been derived [26, 41].

Algorithm (34.38) exhibits a p-th order of convergence. That is, the following relation holds [26]

$$\frac{\|\boldsymbol{x}_k - \boldsymbol{x}^+\|}{\|\boldsymbol{x}^+\|} \leq c^{p^k} \,, \tag{34.39}$$

where the convergence factor c is described by Eq. (34.34).

It is observed that the matrix sequences $\{\Omega_k\}$ and $\boldsymbol{D}_k$ can be computed in advance or *off-line*. When $\boldsymbol{D}$ is block circulant, substantial computational savings result with the use of iteration (34.38) over the linear algorithms. Questions dealing with the best order p of algorithm (34.38) to be used in a given application, as well as comparisons of the trade-off between speed of computation and computational load, are addressed in [26]. One of the drawbacks of the higher order algorithms is that the application of constraints may lead to erroneous results. Combined adaptive or nonadaptive linear and higher order algorithms have been proposed in overcoming this difficulty [11, 26].

34.9 Other Forms of $\Phi(\boldsymbol{x})$

34.9.1 Ill-Posed Problems and Regularization Theory

The two most basic forms of the function $\Phi(\boldsymbol{x})$ have only been considered so far. These two forms are represented by Eqs. (34.22) and (34.26), and are meaningful when the noise in Eq. (34.1) is not taken into account. Without ignoring the noise, however, the solution of Eq. (34.1) represents an ill-posed problem. If the image formation process is modeled in a continuous infinite dimensional space, $\boldsymbol{D}$ becomes an integral operator and Eq. (34.1) becomes a Fredholm integral equation of the first kind. Then the solution of Eq. (34.1) is almost always an ill-posed problem [42, 45, 59, 60]. This means that the unique least-squares solution of minimal norm of (34.1) does not depend continuously on the data, or that a bounded perturbation (noise) in the data results in an unbounded perturbation in the solution, or that the generalized inverse of $\boldsymbol{D}$ is unbounded [42]. The integral operator $\boldsymbol{D}$ has a countably infinite number of singular values that can be ordered with their limit approaching zero [42]. Since the finite dimensional discrete problem of image restoration results from the discretization of an ill-posed continuous problem, the matrix $\boldsymbol{D}$ has (in addition to possibly a number of zero singular values) a cluster of very small singular values. Clearly, the finer the discretization (the larger the size of $\boldsymbol{D}$) the closer the limit of the singular values is approximated. Therefore, although the finite dimensional inverse problem is well posed in the least-squares sense [42], the ill-posedness of the continuous problem translates into an ill-conditioned matrix $\boldsymbol{D}$.

A regularization method replaces an ill-posed problem by a well-posed problem, whose solution is an acceptable approximation to the solution of the given ill-posed problem [39, 56]. In general, regularization methods aim at providing solutions which preserve the fidelity to the data but also satisfy our prior knowledge about certain properties of the solution. A class of regularization methods associates both the class of admissible solutions and the observation noise with random processes [12]. Another class of regularization methods regards the solution as a deterministic quantity. We give examples of this second class of regularization methods in the following.

34.9.2 Constrained Minimization Regularization Approaches

Most regularization approaches transform the original inverse problem into a constrained optimization problem. That is, a functional needs to be optimized with respect to the original image and possibly other parameters. By using the necessary condition for optimality, the gradient of the functional with respect to the original image is set equal to zero, therefore determining the mathematical form of $\Phi(\boldsymbol{x})$. The successive approximations iteration becomes in this case a gradient method with a fixed step (determined by β). We briefly mention next the general form of some of the commonly used functionals.

Set Theoretic Formulation

With this approach the problem of solving Eq. (34.1) is replaced by the problem of searching for vectors $\boldsymbol{x}$ which belong to both sets [21, 25, 27]

$$\|\boldsymbol{D}\boldsymbol{x} - \boldsymbol{y}\| \leq \epsilon \,, \tag{34.40}$$

and

$$\|\boldsymbol{C}\boldsymbol{x}\| \leq E \,, \tag{34.41}$$

where ϵ is an estimate on the data accuracy (noise norm), E a prescribed constant, and $\boldsymbol{C}$ a high-pass operator. Inequality (34.41) constrains the energy of the signal at high frequencies, therefore requiring that the restored signal is smooth. On the other hand, inequality (34.40) requires that the fidelity to the available data is preserved.

Inequalities (34.40) and (34.41) can be respectively rewritten as [25, 27]

$$\left(\boldsymbol{x} - \boldsymbol{x}^{+}\right)^{T} \frac{\boldsymbol{D}^{T}\boldsymbol{D}}{\epsilon^{2}} \left(\boldsymbol{x} - \boldsymbol{x}^{+}\right) \leq 1 \,, \tag{34.42}$$

and

$$\boldsymbol{x}^{T} \frac{\boldsymbol{C}^{T}\boldsymbol{C}}{E_{2}} \boldsymbol{x} \leq 1 \,, \tag{34.43}$$

where $\boldsymbol{x}^{+} = \boldsymbol{D}^{+}\boldsymbol{y}$. That is, each of them represents an N-dimensional ellipsoid, where N is the dimensionality of the vectors involved. The intersection of the two ellipsoids (assuming it is not empty) is also a convex set but not an ellipsoid. The center of one of the ellipsoids which bounds the intersection can be chosen as the solution to the problem [50]. Clearly, even if the intersection is not empty, the center of the bounding ellipsoid may not belong to the intersection, and, therefore, a posterior test is required. The equation the center of one of the bounding ellipsoids is satisfying is given by [25, 27]

$$\Phi(\boldsymbol{x}) = \left(\boldsymbol{D}^{T}\boldsymbol{D} + \alpha \boldsymbol{C}^{T}\boldsymbol{C}\right)\boldsymbol{x} - \boldsymbol{D}^{T}\boldsymbol{y} = 0 \,, \tag{34.44}$$

where α, the *regularization parameter*, is equal to $(\epsilon/E)^2$.

Projection Onto Convex Sets (POCS) Approach

Iteration (34.37) can also be applied in finding a solution which belongs to both ellipsoids (34.42) and (34.43). The respective projections $P_1\boldsymbol{x}$ and $P_2\boldsymbol{x}$ are defined by [25]

$$\mathbf{P}_1\boldsymbol{x} = \boldsymbol{x} + \lambda_1(\mathbf{I} + \lambda_1\boldsymbol{D}^{T}\boldsymbol{D})^{-1}\boldsymbol{D}^{T}(\boldsymbol{y} - \boldsymbol{D}\boldsymbol{x}) \tag{34.45}$$

$$\mathbf{P}_2\boldsymbol{x} = [\mathbf{I} - \lambda_2(\mathbf{I} + \lambda_2\boldsymbol{C}^{T}\boldsymbol{C})^{-1}\boldsymbol{C}^{T}\boldsymbol{C}]\boldsymbol{x}, \tag{34.46}$$

where λ_1 and λ_2 need to be chosen so that conditions (34.42) and (34.43) are satisfied, respectively. Clearly, a number of other projection operators can be used in (34.37) which force the signal to exhibit certain known *a priori* properties expressed by convex sets.

A Functional Minimization Approach

The determination of the value of the regularization parameter is a critical issue in regularized restoration. A number of approaches for determining its value are presented in [13]. If only one of the parameters ϵ or E in (34.40) and (34.41) is known, a constrained least-squares formulation can be followed [9, 15]. With it, the size of one of the ellipsoids is minimized, subject to the constraint that the solution belongs to the surface of the other ellipsoid (the one defined by the known parameter). Following the Lagrangian approach, which transforms the constrained optimization problem into an unconstrained one, the following functional is minimized

$$M(\alpha, \boldsymbol{x}) = \|\boldsymbol{Dx} - \boldsymbol{y}\|^2 + \alpha\|\boldsymbol{Cx}\|^2 \; . \tag{34.47}$$

The necessary condition for a minimum is that the gradient of $M(\alpha, \boldsymbol{x})$ is equal to zero. That is, in this case

$$\Phi(\boldsymbol{x}) = \nabla_{\boldsymbol{x}} M(\alpha, \boldsymbol{x}) = \left(\boldsymbol{D}^T\boldsymbol{D} + \alpha\boldsymbol{C}^T\boldsymbol{C}\right)\boldsymbol{x} - \boldsymbol{D}^T\boldsymbol{y} \; , \tag{34.48}$$

which is identical to (34.44), with the only difference that α now is not known, but needs to be determined.

Spatially Adaptive Iteration

Spatially adaptive image restoration is the next natural step in improving the quality of the restored images. There are various ways to argue the introduction of spatial adaptivity, the most commonly used ones being the nonhomogeneity or nonstationarity of the image field and the properties of the human visual system. In either case, the functional to be minimized takes the form [22, 23, 34]

$$M(\alpha, \boldsymbol{x}) = \|\boldsymbol{Dx} - \boldsymbol{y}\|^2_{\boldsymbol{W}_1} + \alpha\|\boldsymbol{Cx}\|^2_{\boldsymbol{W}_2} \; , \tag{34.49}$$

in which case

$$\Phi(\boldsymbol{x}) = \nabla_{\boldsymbol{x}} M(\alpha, \boldsymbol{x}) = \left(\boldsymbol{D}^T\boldsymbol{W}_1^T\boldsymbol{W}_1\boldsymbol{D} + \alpha\boldsymbol{C}^T\boldsymbol{W}_2^T\boldsymbol{W}_2\boldsymbol{C}\right)\boldsymbol{x} - \boldsymbol{D}^T\boldsymbol{W}_1\boldsymbol{y} \; . \tag{34.50}$$

The choice of the diagonal weighting matrices $\boldsymbol{W}_1$ and $\boldsymbol{W}_2$ can be justified in various ways. In [16, 22, 23, 25] both matrices are determined by the noise visibility matrix $\boldsymbol{V}$ [2, 46]. That is, $\boldsymbol{W}_1 = \boldsymbol{V}^T\boldsymbol{V}$ and $\boldsymbol{W}_2 = \mathbf{I} - \boldsymbol{V}^T\boldsymbol{V}$. The entries of $\mathbf{V}$ take values between 0 and 1. They are equal to 0 at the edges (noise is not visible), equal to 1 at the flat regions (noise is visible) and take values in between at the regions with moderate spatial activity. A study of the mapping between the level of spatial activity and the values of the visibility function appears in [11]. The weighting matrices can also be defined by considering the relationship of the restoration approach presented here to the MAP restoration approach [30]. Then, the weighting matrices $\boldsymbol{W}_1$ and $\boldsymbol{W}_2$ contain information about the nonstationarity and/or the nonwhiteness of the high-pass filtered image and noise, respectively.

Robust Functionals

Robust functionals can be employed for the representation of both the noise and the signal statistics. They allow for the efficient suppression of a wide variety of noise processes and permit the reconstruction of sharper edges than their quadratic counterparts. In a robust set-theoretic set-up a solution is sought by minimizing [65]

$$M(\alpha, \boldsymbol{x}) = R_n(\boldsymbol{y} - \boldsymbol{Dx}) + \alpha R_x(\boldsymbol{Cx}) \; . \tag{34.51}$$

$R_n()$ and $R_x()$ are referred to as the residual and stabilizing functionals, respectively, and they are defined in terms of their *kernel functions*. The derivative of the kernel function is called the *influence function*.

$\Phi(\boldsymbol{x})$ in this case equals the gradient of $M(\alpha, \boldsymbol{x})$ in Eq. (34.51). A large number of robust functionals have been proposed in the literature. The properties of potential functions to be used in robust Bayesian estimation are listed in [35]. A robust maximum absolute entropy and a robust minimum absolute-information functionals are introduced in [65]. Clearly since the functionals $R_n()$ and $R_x()$ are typically nonlinear and may not be convex, the convergence analysis of iteration (34.21) or (34.36) is considerably more complicated.

34.9.3 Iteration Adaptive Image Restoration Algorithms

As it has become clear by now there are various pieces of information needed by any regularization algorithms in determining the unknown parameters. In the context of deterministic regularization, the most commonly needed parameter is the regularization parameter. Its determination depends on the noise statistics and the properties of the image. With the set theoretic regularization approach, it is required that the original image is smooth, in which case a bound on the energy of the high-pass filtered image is needed. This bound is proportional to the variance of the image in a stochastic context. In addition, knowledge of the noise variance is also required. In a MAP framework such parameters are called *hyperparameters* [8, 40]. Clearly, such parameters are not typically available and need to be estimated from the available noisy and blurred data. Various techniques for estimating the regularization parameter are discussed, for example, in [13].

In the following we briefly describe a new paradigm we have introduced in the context of iterative image restoration algorithms [18, 19, 20, 29, 30]. According to it, the required information by the deterministic regularization approach is updated at each restoration step, based on the partially restored image.

Spatially Adaptive Algorithm

For the spatially adaptive algorithm we mentioned above, the proposed general form of the weighted smoothing functional whose minimization will result in a restored image is written as

$$\begin{aligned} M_w\left(\lambda_w(\boldsymbol{x}), \boldsymbol{x}\right) &= \|\boldsymbol{y} - \boldsymbol{D}\boldsymbol{x}\|^2_{\boldsymbol{A}(\boldsymbol{x})} + \lambda_w(\boldsymbol{x})\|\boldsymbol{C}\boldsymbol{x}\|^2_{\boldsymbol{B}(\boldsymbol{x})} \\ &= \|\boldsymbol{n}\|^2_{\boldsymbol{A}(\boldsymbol{x})} + \lambda_w(\boldsymbol{x})\|\boldsymbol{C}\boldsymbol{x}\|^2_{\boldsymbol{B}(\boldsymbol{x})}, \end{aligned} \tag{34.52}$$

where the weighting matrices $\boldsymbol{A}(\boldsymbol{x})$ and $\boldsymbol{B}(\boldsymbol{x})$, both functions of the original image, are used to incorporate noise and image characteristics into the restoration process, respectively. The regularization parameter, also a function of $\boldsymbol{x}$, is defined in such a way as to make the smoothing functional in (34.52) convex with a unique global minimizer.

One of the $\lambda_w(\boldsymbol{x})$ we have proposed is given by

$$\lambda_w(\boldsymbol{x}) = \frac{\|\boldsymbol{y} - \boldsymbol{D}\boldsymbol{x}\|^2_{\boldsymbol{A}(\boldsymbol{x})}}{(1/\gamma) - \|\boldsymbol{C}\boldsymbol{x}\|^2_{\boldsymbol{B}(\boldsymbol{x})}}, \tag{34.53}$$

where the parameter γ is determined from the convergence and convexity analyses.

The main objective with this approach is to employ an iterative algorithm to estimate the regularization parameter and the proper weighting matrices at the same time with the restored image. The available estimate of the restored image at each iteration step will be used for determining the value of the regularization parameter. That is, the regularization parameter is defined as a function of the original image (and eventually in practice of an estimate of it). Of great importance is the form of this functional, so that the smoothing functional to be minimized preserves its convexity and exhibits a global minimizer. $\lambda_w(\boldsymbol{x})$ maps a vector $\boldsymbol{x}$ onto the positive real line. Its purpose is as before to control the relative contribution of the error term $\|\boldsymbol{y} - \boldsymbol{D}\boldsymbol{x}\|^2_{\boldsymbol{A}(\boldsymbol{x})}$, which enforces "faithfulness" to the data, and the stabilizing functional $\|\boldsymbol{Cx}\|^2_{\boldsymbol{B}(\boldsymbol{x})}$, which enforces smoothness on the solution. Its dependency, however, on the original image, as well as the available data, is explicitly utilized. This dependency on the other hand is implicitly utilized in the constrained least-squares approach, according to which the minimization of $M_w(\lambda_w(\boldsymbol{x}), \boldsymbol{x})$ and the determination of the regularization parameter $\lambda_w(\boldsymbol{x})$ are completely separate steps. The desired properties of $\lambda_w(\boldsymbol{x})$ and $M_w(\lambda_w(\boldsymbol{x}), \boldsymbol{x})$ are analyzed in [20]. The relationship of the resulting forms to the hierarchical Bayesian approach towards image restoration and estimation of the regularization parameters is explored in [40].

In this case, therefore, $\Phi(\boldsymbol{x}) = \nabla_{\boldsymbol{x}} M_w(\lambda_w(\boldsymbol{x}), \boldsymbol{x})$. The successive approximations iteration after some simplifications takes the form [20, 30]

$$\boldsymbol{x}_{k+1} = \boldsymbol{x}_k + \left[\boldsymbol{D}^T \boldsymbol{A}\left(\boldsymbol{x}_k\right) \boldsymbol{y} - \left(\boldsymbol{D}^T \boldsymbol{A}\left(\boldsymbol{x}_k\right) \boldsymbol{D} + \lambda_w\left(\boldsymbol{x}_k\right) \boldsymbol{C}^T \boldsymbol{B}\left(\boldsymbol{x}_k\right) \boldsymbol{C}\right) \boldsymbol{x}_k\right] . \tag{34.54}$$

The information required in defining the regularization parameter and the weights for introducing the spatial adaptivity are defined based on the available information about the restored image at the k-th iteration step. Clearly for all this to make sense the convergence of iteration (34.54) has to be guaranteed. Furthermore, convergence to a unique fixed point, which removes the dependency of the final result on the initial conditions, is also desired. These issues are addressed in detail in [20, 30]. A major advantage of the proposed algorithm is that the convexity of the smoothing functional and the convergence of the resulting algorithm are guaranteed regardless of the choice of the weighting matrices. Another advantage of this algorithm is that the proposed adaptive algorithm simultaneously determines the regularization parameter and the desirable weighting matrices based on the restored image at each iteration step and restores the image, without any prior knowledge.

Frequency Adaptive Algorithm

Adaptivity is now introduced into the restoration process by using a constant smoothness constraint, but by assigning a different regularization parameter at each discrete frequency location. We can now "fine-tune" the regularization of each frequency component, thereby achieving improved results and at the same time speeding up the convergence of the iterative algorithm. The regularization parameters are evaluated simultaneously with the restored image based on the partially restored image.

In this algorithm, the following two ellipsoids $QE_{\boldsymbol{x}}$ and $QE_{\boldsymbol{x}/\boldsymbol{y}}$ are used

$$QE_{\boldsymbol{x}} = \left\{\boldsymbol{x} \mid \; \|\boldsymbol{Cx}\|_{\boldsymbol{R}} \le E_{\boldsymbol{R}}\right\} \tag{34.55}$$

and

$$QE_{\boldsymbol{x}/\boldsymbol{y}} = \left\{\boldsymbol{x} \mid \; \|\boldsymbol{y} - \boldsymbol{Dx}\|_{\boldsymbol{P}} \le \epsilon_{\boldsymbol{P}}\right\} , \tag{34.56}$$

where $\boldsymbol{P}$ and $\boldsymbol{R}$ are both block-circulant weighting matrices. Then a solution which belongs to the intersection of $QE_{\boldsymbol{x}}$ and $QE_{\boldsymbol{x}/\boldsymbol{y}}$ is given by

$$\left(\boldsymbol{D}^T \boldsymbol{P}^T \boldsymbol{P} \boldsymbol{D} + \lambda \boldsymbol{C}^T \boldsymbol{R}^T \boldsymbol{R} \boldsymbol{C}\right) \boldsymbol{x} = \boldsymbol{D}^T \boldsymbol{P}^T \boldsymbol{P} \boldsymbol{y} , \tag{34.57}$$

where $\lambda = (\epsilon_{\mathbf{P}}/E_{\mathbf{R}})^2$. Let us define $\boldsymbol{P}^T\boldsymbol{P} = \boldsymbol{B}$, $\boldsymbol{R} = \boldsymbol{PC}$ and $\lambda \boldsymbol{C}^T \boldsymbol{C} = \boldsymbol{A}$. Then Eq. (34.57) can be written as

$$\boldsymbol{B}\left(\boldsymbol{D}^T \boldsymbol{D} + \boldsymbol{A}\boldsymbol{C}^T \boldsymbol{C}\right) \boldsymbol{x} = \boldsymbol{B}\boldsymbol{D}^T \boldsymbol{y} , \tag{34.58}$$

since all matrices are block-circulant and they therefore commute. The regularization matrix $\boldsymbol{A}$ is defined based on the set theoretic regularization as

$$\boldsymbol{A} = \|\boldsymbol{y} - \boldsymbol{Dx}\|^2 [\|\boldsymbol{Cx}\|^2 \mathbf{I} + \Delta]^{-1} , \tag{34.59}$$

where Δ is a block-circulant matrix used to ensure convergence. $\boldsymbol{B}$ plays the role of the "shaping" matrix [53] for maximizing the speed of convergence at every frequency component as well as for compensating for the near-singular frequency components [19].

With the above formulation, therefore,

$$\Phi(\boldsymbol{x}) = \boldsymbol{B}\left(\left(\boldsymbol{D}^T\boldsymbol{D} + \boldsymbol{A}\boldsymbol{C}^T\boldsymbol{C}\right)\boldsymbol{x} - \boldsymbol{D}^T\boldsymbol{y}\right) , \tag{34.60}$$

and the successive approximations iteration (34.21) becomes

$$\boldsymbol{x}_{k+1} = \boldsymbol{x}_k + \boldsymbol{B}\left[\boldsymbol{D}^T\boldsymbol{y} - \left(\boldsymbol{D}^T\boldsymbol{D} + \boldsymbol{A}_k\boldsymbol{C}^T\boldsymbol{C}\right)\boldsymbol{x}_k\right] , \tag{34.61}$$

where $\boldsymbol{A}_k = \|\boldsymbol{y} - \boldsymbol{D}\boldsymbol{x}_k\|^2[\|\boldsymbol{C}\boldsymbol{x}_k\|^2\mathbf{I} + \Delta_k]^{-1}$. It is mentioned here that iteration (34.61) can also be derived from the regularized equation

$$\left(\boldsymbol{D}^T\boldsymbol{D} + \boldsymbol{A}\boldsymbol{C}^T\boldsymbol{C}\right)\boldsymbol{x} = \boldsymbol{D}^T\boldsymbol{y} , \tag{34.62}$$

using the generalized Landweber's iteration [53]. Since all matrices in iteration (34.61) are block-circulant, the iteration can be written in the discrete frequency domain as

$$X_{k+1}(\underline{p}) = X_k(\underline{p}) + \beta(\underline{p})\left[D^*(\underline{p})Y(\underline{p}) - \left(|D(\underline{p})|^2 + \lambda_k(\underline{p})|C(\underline{p})|^2\right)X_k(\underline{p})\right] , \tag{34.63}$$

where $\underline{p} = (p_1, p_2)$, $0 \le p_1 \le N-1$, $0 \le p_2 \le N-1$, $X_{k+1}(\underline{p})$ and $Y(\underline{p})$ represent the 2D DFT of the unstacked image estimate $\boldsymbol{x}_{k+1}$, and the noisy-blurred image $\boldsymbol{y}$ and $D(\underline{p})$, $C(\underline{p})$, $\beta(\underline{p})$, and $\lambda_k(\underline{p})$ represent 2D DFTs of the 2D sequences which form the block-circulant matrices $\boldsymbol{D}$, $\boldsymbol{C}$, $\boldsymbol{B}$, and $\boldsymbol{A}_k$, respectively. Since Δ_k is block-circulant $\lambda_k(\underline{p})$ is given by

$$\lambda_k(\underline{p}) = \frac{\sum_m |Y(\underline{m}) - D(\underline{m})X_k(\underline{m})|^2}{\sum_n |C(\underline{n})X_k(\underline{n})|^2 + \delta_k(\underline{p})} , \tag{34.64}$$

where $\delta_k(\underline{p})$ is the 2D DFT of the sequence which forms Δ_k.

The allowable range of each regularization and control parameter and the convergence analysis of the iterative algorithm are developed in detail in [19]. It is shown that the algorithm has more than two fixed points. The first fixed point is the inverse or generalized inverse solution of Eq. (34.58). The second type of fixed points are regularized approximations to the original image. Since there is more than one solution to iteration (34.63), the determination of the initial condition becomes important. It has been verified experimentally [19] that if a "smooth" image is used for $X_0(\underline{p})$ almost identical fixed points result independently of X_0. The use of spectral filtering functions [53] is also incorporated into the iteration, as shown in [19].

34.10 Discussion

In this chapter we briefly described the application of the successive approximations-based class of iterative algorithms to the problem of restoring a noisy and blurred signal. We analyzed in some detail the simpler forms of the algorithm, while making reference to work which deals with more complicated forms of the algorithms. There are obviously a number of algorithms and issues pertaining to such algorithms which have not been addressed at all. For example, iterative algorithms with a varying relaxation parameter β, such as the steepest descent and conjugate gradient methods, can be applied to the image restoration problem [4, 37]. The number of iterations also represents a means for regularizing the restoration problem [55, 58]. Iterative algorithms which depend on more than one previous restoration steps (multi-step algorithms) have also been considered, primarily for implementation reasons [24].

It is the hope and the expectation of the author that the material presented will form a good introduction to the topic for the engineer or the graduate student who would like to work in this area.

References

[1] Abbiss, J.B., DeMol, C., and Dhadwal, H.S., Regularized iterative and noniterative procedures for object restoration from experimental data, *Opt. Acta*, 107-124, 1983.

[2] Anderson, G.L. and Netravali, A.N., Image restoration based on a subjective criterion, *IEEE Trans. Sys. Man. Cybern.*, SMC-6: 845-853, Dec., 1976.

[3] Andrews, H.C. and Hunt, B.R., *Digital Image Restoration*, Prentice-Hall, Englewood Cliffs, NJ, 1977.

[4] Angel, E.S. and Jain, A.K., Restoration of images degraded by spatially varying point spread functions by a conjugate gradient method, *Appl. Opt.*, 17: 2186-2190, July, 1978.

[5] Banham, M. and Katsaggelos, A.K., Digital image restoration, *Signal Processing Mag.*, 14(2), 24–41, Mar., 1997.

[6] Bialy, H., Iterative Behandlung Linearen Funktionalgleichungen, *Arch. Ration. Mech. Anal.*, 4: 166-176, July, 1959.

[7] Biemond, J., Lagendijk, R.L., and Mersereau, R.M., Iterative methods for image deblurring, *Proc. IEEE*, 78(5): 856-883, May, 1990.

[8] Demoment, G., Image reconstruction and restoration: overview of common estimation structures and problems, *IEEE Trans. Acoust. Speech Signal Process.*, 37(12): 2024-2036, Dec., 1989.

[9] Dines, K.A. and Kak, A.C., Constrained least squares filtering, *IEEE Trans. Acoust. Speech Signal Process.*, ASSP-25: 346-350, 1977.

[10] Dudgeon, D.E. and Mersereau, R.M., *Multidimensional Digital Signal Processing*, Prentice-Hall, Englewood Cliffs, NJ, 1984.

[11] Efstratiadis, S.N. and Katsaggelos, A.K., Adaptive iterative image restoration with reduced computational load, *Opt. Eng.*, 29: 1458-1468, Dec., 1990.

[12] Franklin, J.N., Well-posed stochastic extentions of ill-posed linear problems, *J. Math. Anal.*, 31: 682-716, 1970.

[13] Galatsanos, N.P. and Katsaggelos, A.K., Methods for choosing the regularization parameter and estimating the noise variance in image restoration and their relation, *IEEE Trans. Image Process.*, 1: 322-336, July, 1992.

[14] Huang, T.S., Barker, D.A., and Berger, S.P., Iterative image restoration, *Appl. Opt.*, 14: 1165-1168, May, 1975.

[15] Hunt, B.R., The application of constrained least squares estimation to image restoration by digital computers, *IEEE Trans. Comput.*, C-22: 805-812, Sept., 1973.

[16] Ichioka, Y. and Nakajima, N., Iterative image restoration considering visibility, *J. Opt. Soc. Am.*, 71: 983-988, Aug., 1981.

[17] Jansson, P.A., Hunt R.H., and Pyler, E.K., Resolution enhancement of spectra, *J. Opt. Soc. Am.*, 60: 596-599, May, 1970.

[18] Kang, M.G. and Katsaggelos, A.K., Iterative image restoration with simultaneous estimation of the regularization parameter, *IEEE Trans. Signal Process.*, 40(9): 2329-2334, Sept., 1992.

[19] Kang, M.G. and Katsaggelos, A.K., Frequency domain adaptive iterative image restoration and evaluation of the regularization parameter, *Opt. Eng.*, 33(10): 3222-3232, Oct., 1994.

[20] Kang, M.G. and Katsaggelos, A.K., General choice of the regularization functional in regularized image restoration, *IEEE Trans. Image Process.*, 4(5): 594-602, May, 1995.

[21] Katsaggelos, A.K., Biemond, J., Mersereau, R.M., and Schafer, R.W., A general formulation of constrained iterative restoration algorithms, *Proc. 1985 Int. Conf. Acoust. Speech Signal Process.*, pp. 700-703, Tampa, FL, March, 1985.

[22] Katsaggelos, A.K., Biemond, J., Mersereau, R.M., and Schafer, R.W., Nonstationary iterative image restoration, *Proc. 1985 Int. Conf. Acoust. Speech Signal Process.*, pp. 696-699, Tampa, FL, March, 1985.

[23] Katsaggelos, A.K., A general formulation of adaptive iterative image restoration algorithms, *Proc. 1986 Conf. Inf. Sciences Syst.*, pp. 42-47, Princeton, NJ, March, 1986.

[24] Katsaggelos, A.K. and Kumar, S.P.R., Single and multistep iterative image restoration and VLSI implementation, *Signal Process.*, 16(1): 29-40, Jan., 1989.

[25] Katsaggelos, A.K., Iterative image restoration algorithm, *Opt. Eng.*, 28(7): 735-748, July, 1989.

[26] Katsaggelos, A.K. and Efstratiadis, S.N., A class of iterative signal restoration algorithms, *IEEE Trans. Acoust. Speech Signal Process.*, 38: 778-786, May, 1990 (reprinted in *Digital Image Processing*, R. Chellappa, Ed., IEEE Computer Society Press).

[27] Katsaggelos, A.K., Biemond, J., Mersereau, R.M., and Schafer, R.W., A regularized iterative image restoration algorithm, *IEEE Trans. Signal Process.*, 39(4): 914-929, April, 1991.

[28] Katsaggelos, A.K., Ed., *Digital Image Restoration*, Springer Series in Information Sciences, vol. 23, Springer-Verlag, Heidelberg, 1991.

[29] Katsaggelos, A.K. and Kang, M.G., Iterative evaluation of the regularization parameter in regularized image restoration, *J. Vis. Commun Image Rep.*, special issue on *Image Restoration*, vol. 3, no. 6, pp. 446-455, Dec., 1992.

[30] Katsaggelos, A.K. and Kang, M.G., A spatially adaptive iterative algorithm for the restoration of astronomical images, *Int. J. Imag. Syst. Technol.*, special issue on *Image Reconstruction and Restoration in Astronomy*, vol. 6, no. 4, pp. 305-313, winter, 1995.

[31] Kawata, S., Ichioka, Y., and Suzuki, T., Application of man-machine interactive image processing system to iterative image restoration, *Proc. 4th Int. Conf. Patt. Recog.*, pp. 525-529, Kyoto, 1978.

[32] Kawata, S. and Ichioka, Y., Iterative image restoration for linearly degraded images, I. Basis, *J. Opt. Soc. Am.*, 70: 762-768, July, 1980.

[33] Kawata, S. and Ichioka, Y., Iterative image restoration for linearly degraded images, II. Reblurring procedure, *J. Opt. Soc. Am.*, 70: 768-772, July, 1980.

[34] Lagendijk, R.L., Biemond, J., and Boekee, D.E., Regularized iterative image restoration with ringing reduction, *IEEE Trans. Acoust. Speech Signal Process.*, 36: 1804-1887, Dec., 1988.

[35] Lange, K., Convergence of EM image reconstruction algorithms with Gibbs smoothing, *IEEE Trans. Med. Imag.*, 9(4), Dec., 1990.

[36] Mammone, R.J., *Computational Methods of Signal Recovery and Recognition*, Wiley, 1992.

[37] Marucci, R., Mersereau, R.M., and Schafer, R.W., Constrained iterative deconvolution using a conjugate gradient algorithm, *Proc. 1982 IEEE Int. Conf. Acoust. Speech Signal Process.*, pp. 1845-1848, Paris, France, May, 1982.

[38] Mersereau, R.M. and Schafer, R.W., Comparative study of iterative deconvolution algorithms, *Proc. 1978 IEEE Int. Conf. Acoust. Speech Signal Process.*, pp. 192-195, April, 1978.

[39] Miller, K., Least-squares method for ill-posed problems with a prescribed bound, *SIAM J. Math. Anal.*, 1: 52-74, Feb., 1970.

[40] Molina, R. and Katsaggelos, A.K., The hierarchical approach to image restoration and the iterative evaluation of the regularization parameter, *Proc. 1994 SPIE Conf. Vis. Commun. Image Process.*, pp. 244-251, Chicago, IL, Sept., 1994.

[41] Morris, C.E., Richards M.A., and Hayes, M.H., Fast reconstruction of linearly distorted signals, *IEEE Trans. Acoust. Speech Signal Process.*, 36: 1017-1025, July, 1988.

[42] Nashed, M.Z., Operator theoretic and computational approaches to ill-posed problems with application to antenna theory, *IEEE Trans. Ant. Prop.*, AP-29: 220-231, March, 1981.

[43] Ortega, J.M. and Rheinboldt, W.C., *Iterative Solution of Nonlinear Equations in Several Variables*, Academic Press, New York, 1970.

[44] Ortega, J.M., *Numerical Analysis: A Second Course*, Academic Press, New York, 1972.

[45] Phillips, D.L., A technique for the numerical solution of certain integral equations of the first kind, *Assoc. Comp. Mach.*, 9: pp. 84-97, 1962.

[46] Rajala, S.S. and DeFigueiredo, R.J.P., Adaptive nonlinear image restoration by a modified Kalman filtering approach, *IEEE Trans. Acoust. Speech Signal Process.*, ASSP-29: Oct., 1981.

[47] Richards, M.A., Schafer, R.W., and Mersereau, R.M., An experimental study of the effects of noise on a class of iterative deconvolution algorithms, *Proc. 1979 Int. Conf. Acoust. Speech Signal Process.*, pp. 401-404, April, 1979.

[48] Sanz J.L.C. and Huang, T.S., Iterative Time-Limited Signal Restoration, *IEEE Trans. Acoust. Speech Signal Processing*, ASSP-31: 643-649, June, 1983.

[49] Schafer, R. W., Mersereau, R.M., and Richards, M.A., Constrained iterative restoration algorithms, *Proc. IEEE*, 69: 432-450, April, 1981.

[50] Schweppe, F.C., *Uncertain Dynamic Systems*, Prentice-Hall, 1973.

[51] Sondhi, M.M., Image restoration: the removal of spatially invariant degredations, *Proc. IEEE*, vol. 60, pp. 842-853, July, 1972.

[52] Stark, H., *Image Recovery: Theory and Applications*, Academic Press, New York, 1987.

[53] Strand, O.N., Theory and methods related to the singular-function expansion and Landweber's iteration for integral equations of the first kind, *SIAM J. Numerical Anal.*, 11: 798-825, Sept., 1974.

[54] Strang, G., *Linear Algebra and Its Applications*, 2nd ed., Academic Press, New York, 1980.

[55] Sullivan, B.J. and Katsaggelos, A.K., A new termination rule for linear iterative image restoration algorithms, *Opt. Eng.*, 29: 471-477, May, 1990.

[56] Tikhonov, A.N. and Arsenin, V.Y., *Solution of Ill-Posed Problems*, Winston, Wiley, 1977.

[57] Tom, V.T., Quatieri, T.F., Hayes, M.H., and McClellan, J.M., Convergence of iterative nonexpansive signal reconstruction algorithms, *IEEE Trans. Acoust. Speech Signal Process.*, ASSP-29: 1052-1058, Oct., 1981.

[58] Trussell, H.J., Convergence criteria for iterative restoration methods, *IEEE Trans. Acoust. Speech Signal Process.*, ASSP-31: 129-136, Feb., 1983.

[59] Twomey, S., On the numerical solution of Fredholm integral equations of the first kind by the inversion of the linear system produced by quadrature, *Assoc. Comp. Mach.*, 10: 97-101, 1963.

[60] Twomey, S., The application of numerical filtering of the solution of integral equations encountered in indirect sensing measurements, *J. Franklin Inst.*, 279: 95-109, Feb., 1965.

[61] Van Citttert, P.H., Zum Einfluss der Spaltbreite auf die Intensitatswerteilung in Spektrallinien II, *Z. Physik*, 69: 298-308, 1931.

[62] Yang, Y., Galatsanos N.P., and Katsaggelos, A.K., Regularized image reconstruction from incomplete block discrete cosine transform data, *IEEE Trans. Circuits Syst. Video Technol.*, 3(6): 421-432, Dec., 1993.

[63] Yang, Y., Galatsanos N.P., and Katsaggelos, A.K., Set theoretic spatially-adaptive reconstruction of block transform compressed images, *IEEE Trans. Image Process.*, 4(7): 896-908, July, 1995.

[64] Youla, D.C. and Webb, H., Image reconstruction by the method of convex projections, Pt. 1-Theory, *IEEE Trans. Med. Imag.*, MI-1(2): 81-94, Oct., 1982.

[65] Zervakis, M.E., Katsaggelos, A.K., and Kwon, T.M., A class of robust entropic functionals for image restoration, *IEEE Trans. Image Process.*, 4(6): 752-773, June, 1995.